# An Evaluation of the One-Dimensional Turbulence Model: Comparison with Direct Numerical Simulations of $CO/H_2$ Jets with Extinction and Reignition

Naveen Punati[a], James C. Sutherland[a], Alan R. Kerstein[b], Evatt R. Hawkes[c], Jacqueline H. Chen[b]

[a]*The University of Utah, Salt Lake City, UT, 84112*
[b]*Sandia National Laboratories, Livermore, CA, 94550*
[c]*The University of New South Wales, Sydney, NSW 2052, Australia*

**Abstract**

A variant of the One-Dimensional Turbulence (ODT) model formulated in an Eulerian reference frame is applied to a planar nonpremixed turbulent jet flame and results from the model prediction are compared with DNS data. The model employed herein solves the full set of conservation equations for mass, momentum, energy, and species on a one-dimensional domain corresponding to the transverse jet direction. The effects of turbulent mixing are modeled via a stochastic process, while the full range of diffusive-reactive length and time scales are resolved directly on the one-dimensional domain. A detailed chemical mechanism consisting of 11 species and 21 reactions and mixture averaged transport is used in this study (consistent with DNS simulations). Comparisons between the model and DNS data in physical and state space are shown, including conditional statistics. Results indicate that the model accurately reproduces the DNS data set. Turbulence-chemistry interactions, including trends for extinction and re-ignition, are captured by the model. Differences observed between model prediction and data are the result of early excess extinction observed in the model. The reasons for the early extinction are discussed within the model context.

*Keywords:* turbulent nonpremixed jet flame, direct numerical simulation, one-dimensional turbulence, extinction, re-ignition

## 1. Introduction

Predictive methods based on fundamental principles to model turbulence-chemistry interactions are important in turbulent reacting flow simulations to improve combustion efficiency and to reduce emissions. The existence of a wide range of length and time scales in high Reynolds number flows makes Direct Numerical Simulations (DNS) computationally intractable [1]. To reduce the computational cost one generally averages or filters the governing equations to remove fine scales as in the Reynolds-Averaged Navier-Stokes (RANS) and Large eddy simulation (LES) approaches. These averaged equations are coupled with turbulent combustion models to address the non-linear nature of chemical reactions occurring at molecular mixing scales (fine scales).

Turbulent combustion models can be broadly categorized into moment methods and probability density function (PDF) approaches [2]. In moment methods, molecular transport is explicitly represented and a reduced parameter space approach is adopted for the solution of reacting scalars and their associated source terms. For PDF approaches, chemical source terms appear in closed form whereas mixing is implemented stochastically using a mixing model. The linear-eddy model, developed by Kerstein [3–5], is one such stochastic mixing model which has been used as an alternative strategy for closure in turbulent combustion [6–8].

The One-Dimensional Turbulence model (ODT) is an outgrowth of the LEM model that incorporates desirable aspects of both these classes of models by solving unfiltered governing equations in one spatial dimension with a stochastic model for turbulence [9]. The ODT model can be considered to be a complete turbulence model in contrast with LEM, a mixing model. In ODT, one or more velocity components are transported and are used to determine the eddy frequency and eddy-size distribution, enabling a mechanism for driving turbulence. As a stand-alone model, ODT has been successfully applied to simulate homogeneous turbulent non-reacting [9–16] and reacting flows [17–20]. However for stand-alone modeling of turbulent flows using either LEM or ODT, one must define the dominant direction of mean property variation *a priori*. For more complex flows which may not have a single dominant direction, ODT has been used as a subgrid scale model in both RANS [18, 21] and LES [22] to provide closure for reacting scalars in combustion.

The ODT formulations (traditional approaches) discussed so far solve the governing equations in a Lagrangian reference frame. For the stand-alone modeling of reacting jets, temporally developing equations are solved and ODT domain is advected in a Lagrangian manner to provide an approximate mapping between space and time [17]. This mapping is used to validate the model prediction against spatially developing turbulent jet flames. Recently, a variant of the existing ODT model in an Eulerian reference frame has been developed and applied to non-reacting and reacting jets [23, 24].

The main objective of the present study is to perform stand-alone Eulerian ODT simulations for a nonpremixed temporally developing planar syngas jet flame and to compare the model prediction with DNS data [25, 26]. This work is the first

time that a stand-alone ODT model has been compared directly with 3D DNS data for a reacting flow, and also demonstrates the richness of the data the model can produce. It also represents one of the first attempts to model the DNS data set, the only other approach to date being a combination of LEM with LES [27]. In the present work, all simulation details, including mesh spacing, initial conditions, boundary conditions, and thermodynamic, chemical kinetc and transport models were matched with the DNS.

The paper is organized as follows. First we present the governing equations that are solved and discuss some of the important differences between traditional approaches and the model used for the current study. We then evaluate the model's capability to reproduce finite-rate chemistry effects such as extinction and re-ignition. Flow entrainment effects are presented using axial statistics for velocity and mixture fraction. Conditional statistics of species and probability density functions of temperature and scalar dissipation are presented.

## 2. Model Formulation

In ODT, the computational domain is a line of sight through three-dimensional turbulent flow field. The transverse $y$-direction, which is the direction of the most significant gradients (Figure 1), is considered here as the ODT domain. To mimic the three-dimensional nature of turbulence in one spatial dimension, a stochastic process is adopted. The stochastic process consists of a sequence of events, each of which involves transformation of the fields evolving in the flow. For brevity, not all the differences between the traditional approaches and the variant used in the present study are presented here. Complete discussions of the various ODT approaches that describes the similarities and differences between them can be found in [28, 29].

### 2.1. Governing Equations

The ODT model as formulated herein solves the following conservation equation set

$$\frac{\partial \rho}{\partial t} = -\frac{\partial \rho v}{\partial y}, \tag{1}$$

$$\frac{\partial \rho v}{\partial t} = -\frac{\partial \rho v v}{\partial y} - \frac{\partial \tau_{yy}}{\partial y} - \frac{\partial p}{\partial y}, \tag{2}$$

$$\frac{\partial \rho u}{\partial t} = -\frac{\partial \rho v u}{\partial y} - \frac{\partial \tau_{yx}}{\partial y}, \tag{3}$$

$$\frac{\partial \rho e_0}{\partial t} = -\frac{\partial \rho e_0 v}{\partial y} - \frac{\partial p v}{\partial y} - \frac{\partial \tau_{yy} v}{\partial y} - \frac{\partial q}{\partial y}, \tag{4}$$

$$\frac{\partial \rho Y_i}{\partial t} = -\frac{\partial \rho Y_i v}{\partial y} - \frac{\partial J_i}{\partial y} + \omega_i, \tag{5}$$

where $u$ and $v$ refer to streamwise and lateral velocities, $\rho$ is the density, $p$ is the pressure, $\tau$ is the stress tensor, $e_0$ is the total internal energy, $q$ is the heat flux, $Y_i$ is the mass fraction of species $i$, $J_i$ is the species mass diffusive flux, and $\omega_i$ is the reaction rate. These equations are completed with the ideal gas equation of state and constitutive relationships for the diffusive fluxes:

$$\tau_{yy} = -\frac{4}{3}\mu\frac{\partial v}{\partial y}, \tag{6}$$

$$\tau_{yx} = -\mu\frac{\partial u}{\partial y}, \tag{7}$$

$$q = -\lambda\frac{\partial T}{\partial y} + \sum_{i=1}^{n_s} h_i J_i, \tag{8}$$

$$J_i = -\frac{\rho Y_i}{X_i} D_i^{mix}\frac{\partial X_i}{\partial y}, \tag{9}$$

where $\lambda$ is the thermal conductivity, $\mu$ is the viscosity, $T$ is the temperaure, $h_i$ is the enthalpy of species $i$, $D_i^{mix}$ is the mixture-averaged diffusivity for species $i$, and $X_i$ is the mole fraction of species $i$.

This approach differs from previous ODT formulations as it is formulated in an Eulerian frame of reference and thus retains the advective terms accounting for the fluxes in the lateral direction, whereas previous ODT approaches are formulated in a Lagrangian frame of reference where continuity is maintained by modifying the control volumes such that the mass within each volume remains fixed and there is no advective flux through the control volume surfaces. Furthermore, we solve conserved variables (*e.g.* $\rho u$) rather than primitive variables (*e.g.* $u$) as is done in traditional ODT approaches. Finally, we explicitly account for pressure gradients to maintain mass conservation.

### 2.2. Eddy Events

In ODT, the turbulent motions that accelerate mixing are modeled through a series of stochastic rearrangement events. These events may be interpreted as the model analogue of individual turbulent eddies which are referred to as "eddy events" or simply "eddies." Each eddy event interrupts the conserved variables evolution by applying an instantaneous transformation to the fields over some spatial interval $(y_0,\, y_0 + \ell)$, where $y_0$ represents the eddy starting location and $\ell$ is the eddy length.

### 2.3. Triplet Maps

The triplet map forms the heart of any ODT modeling approach, modeling the effects of a three-dimensional eddy with a one-dimensional rearrangement. Triplet maps are qualitatively similar to turbulence in that they have the effect of increasing gradients by redistributing the fluid elements along the 1-D domain. The functional form chosen for the triplet mapping function, $f(y)$, is the simplest of a class of mappings that satisfy the physical requirements of measure preservation, continuity and scale locality over the eddy interval. It can be represented as [9]

$$f(y; y_0, \ell) \equiv y_0 + \begin{cases} 3\,(y - y_0) & y_0 \le y \le y_0 + \frac{1}{3}\ell \\ 2\ell - 3\,(y - y_0) & y_0 + \frac{1}{3}\ell \le y \le y_0 + \frac{2}{3}\ell \\ 3\,(y - y_0) - 2\ell & y_0 + \frac{2}{3}\ell \le y \le y_0 + \ell \\ y - y_0 & \textit{otherwise} \end{cases}. \tag{10}$$

This mapping takes a line segment $[y_0, y_0 + \ell]$ shrinks it to a third of its original length, and then places three copies on the original domain. The middle copy is reversed, which ensures

UU IR Author Manuscript

that property fields remain continuous and introduces the rotational folding effect of turbulent eddy motion. All quantities outside the $[y_0, y_0 + \ell]$ interval are unaffected.

The triplet map is augmented by a "kernel transformation" to implement energy transfers while obeying applicable conservation laws [11]. In the absence of buoyancy, this transformation is needed only when more than one momentum component is defined and energy is transferred between them to emulate pressure-induced energy distribution. For the current formulation, the kernel transformation is

$$(\rho u)_i\,[y] = (\rho u)_i\,[f(y; y_0, \ell)] + c_i K(y), \tag{11}$$

where $(\rho u)_i$ is the $i^{\text{th}}$ component of momentum, $K(y) = y - f(y; y_0, \ell)$, and $c_i$ is a kernel coefficient whose value is determined to guarantee conservation of kinetic energy of component $i$ [24]. Traditional ODT approaches apply triplet maps to velocity rather than momentum. Therefore, for variable density flows, traditional ODT [10] requires an additional kernel, not needed here, to ensure both kinetic energy and momentum conservation.

### 2.4. Eddy Rate Distribution

Similar to the dimensional relationship applied to turbulent eddies, for events defined in ODT a relationship can be formulated between eddy size, energy associated with it and timescale. Given an eddy length scale $\ell$ and turnover time $\tau_e$, $\ell/\tau_e$ is an eddy velocity scale and $\rho\ell^3/\tau_e^2$ is a measure of the kinetic energy of the eddy. We denote $Q_i$ when scaled with $(\rho\ell)$ as the energy associated with $i^{\text{th}}$ velocity component. To determine the eddy turnover time this energy is equated to an appropriate measure of the eddy energy based on the current flow state, which is the available energy of the $i = 2$ (streamwise) velocity component upon completion of eddy implementation, minus an energy penalty that reflects viscous dissipation effects,

$$\left(\frac{\ell}{\tau_e}\right)^2 \sim \frac{(1-\alpha)Q_2 + \alpha\,(Q_1)}{\rho_{avg}\ell} - \mathcal{Z}\frac{\nu_{avg}^2}{\ell^2}. \tag{12}$$

Here, there are two adjustable model parameters: $\mathcal{Z}$ and $\alpha$. $\mathcal{Z}$ represents a "viscous penalty" coefficient, and $\alpha$ controls inter-component energy transfer between velocity components during eddy action. If the eddy energy cannot overcome the viscous dissipation effects then the eddy is disregarded. The energy penalty introduces a threshold Reynolds number that must be exceeded for eddy turnover to occur. The eddy rate distribution governing the occurrence of eddy events during simulated realizations is defined from dimensional reasoning and (12) as

$$\begin{aligned}\lambda &= \frac{C}{\ell^2\tau_e}, \\ &= \frac{C}{\ell^3}\sqrt{\left[\frac{(1-\alpha)\,Q_2 + \alpha\,(Q_1)}{\rho_{avg}\ell}\right] - \mathcal{Z}\frac{\nu_{avg}^2}{\ell^2}}.\end{aligned} \tag{13}$$

where $C$ is an adjustable model parameter representing turbulence intensity.

### 2.5. Large Eddy Suppression

While the viscous cutoff parameter $\mathcal{Z}$ suppresses the least energetic eddies, we require a mechanism to prevent the occurrence of unphysical large eddies. Recall that eddies are implemented as instantaneous events. However, an eddy with a turnover time greater than the elapsed simulation time, $\tau_e > t$ should not physically be admitted. Specifically, eddy events are allowed only when $t \geq \beta\tau_e$, where $\beta$ is a model parameter.

Simultaneous tuning of $\alpha$, $\beta$, $C$ and $\mathcal{Z}$ is needed to simulate a particular flow of interest.

## 3. Computational Configuration

DNS of three-dimensional (3D) temporal planar syngas jet flames with detailed chemistry over a range of jet Reynolds numbers (Re) from 2510 to 9079 have been performed by Hawkes *et. al.* [25, 26]. We consider a case with Re = 4478, which is addressed as Case *M* in the literature. The jet consists of a central fuel stream (50% CO, 10% $H_2$ and 40% $N_2$ by volume) surrounded by counter-flowing oxidizer streams comprised of 25% $O_2$ and 75% $N_2$. The stoichiometric mixture fraction is $Z_{st} = 0.42$ and the steady extinction dissipation rate (based on a steady laminar flamelet calculation) is $\chi_q = 2194\,\text{s}^{-1}$. The fuel and oxidizer stream bulk velocities are $U/2$ and $-U/2$ respectively, with $U = 194$ m/s. The initial fuel stream thickness is $H \approx 0.96$ mm and the characteristic jet time scale, computed using $H/U$, is $t_j \approx 5\ \mu$s. Based on $t_j$, a non-dimensionalized time parameter is defined as $\tau = {}^{t}/_{t_j}$.

The mixture fraction was computed from the local species compositions using Bilger's definition [30], and the scalar dissipation rate is calculated as $\chi = 2D\left(\frac{dZ}{dy}\right)^2$ with $D = {}^{\lambda}/_{(\rho c_p)}$.

Figure 1 illustrates the scalar dissipation rate field of the jet at $\tau = 40$. The DNS data set exhibits significant finite-rate chemistry effects including extinction and re-ignition. Maximum extinction occurs at $\tau \approx 20$, while by $\tau \approx 40$ most of the flame has reignited.

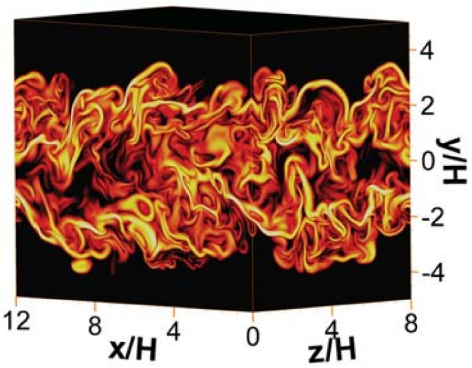


Figure 1: Logarithm of scalar dissipation rate from the DNS[25, 26] at $\tau = 40$ .

The ODT calculations consider a one-dimensional domain aligned with the $y$-direction in Figure 1. The initial conditions for all the variables transported in the ODT model are extracted directly from the DNS data. The detailed chemical mechanism

considered in this study (consisting of 11 species and 21 reactions [25]), temperature and pressure-dependent thermodynamic property evaluation, and the mixture averaged transport treatment are all consistent with the DNS simulations. The spatial and temporal resolution are likewise the same as used in the DNS simulation, with a spatial resolution of 15 $\mu$m and a time step of 2 ns. Simulations are run for 0.25 ms (50 $t_j$) and results are analyzed over 400 ODT simulation realizations. ODT predictions at different times are compared with DNS statistics on $xz$ planes in Figure 1.

## 4. Results & Discussion

### 4.1. Flow Entrainment

The flow entrainment predicted by the ODT model is evaluated by comparing axial evolution of velocity and mixture fraction at different time intervals. The entrainment is sensitive to the choice of ODT parameters (particularly $\beta$ and $C$), which have been tuned to match the spreading rate and decay of the velocity and mixture fraction. The parameter values used in this study are $\alpha = 0.5$, $C = 0.025$, $\beta = 1.0$ and $\mathcal{Z} = 200$. Figure 2 shows comparison of observed and predicted axial evolution of the mean streamwise velocity at $\tau = 6$, 20 and 40. A similar comparison is shown for the mixture fraction in Figure 3. For both velocity and mixture fraction DNS mean values on the left half of the domain are a mirror image of the right half of the domain but for ODT, data at positive and negative $y$ are not combined (*i.e.*, spatial profiles are not symmetrized).

For both velocity and mixture fraction, the decay and spreading rate are very well predicted by the model, demonstrating the model's efficacy in capturing the flow entrainment. The RMS fluctuations in velocity and mixture at different time intervals are also compared with DNS data and included in the supplemental information. The trend exhibited by the ODT model is consistent with the DNS, although the fluctuations predicted by the model are lower than the DNS data.

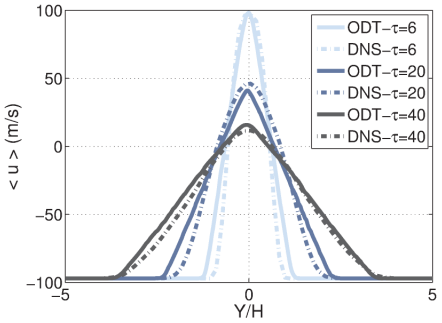


Figure 2: Average streamwise velocity at $\tau = 6$, 20 and 40

### 4.2. Conditional Statistics

Figures 4 and 5 show the mean temperature and OH evolution, respectively, as a function of the mixture fraction at different time intervals. The steady laminar flamelet solution at the

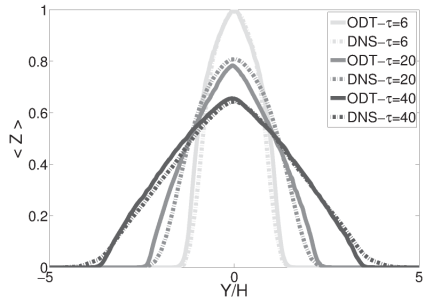


Figure 3: Average mixture fraction profiles at $\tau = 6$, 20 and 40

critical dissipation rate ($\chi_q = 2194\,\mathrm{s}^{-1}$) is also shown for reference. For the case simulated, mixing is initially rapid enough relative to reaction to cause local extinction, which is followed by re-ignition as mixing rates relax. The conditional mean for both temperature and species predicted by ODT is low compared to the DNS data at $\tau = 6$, 20 over the entire mixture fraction range. The ODT model starts predicting local extinction earlier (at $\tau \approx 6$) than the DNS, as indicated by both temperature and OH species mean values dropping close to the extinction limit predicted by the laminar flamelet solution. As the simulation progresses (at $\tau = 20$) the ODT model exhibits stronger extinction than the data as indicated by the low mean values. At $\tau = 40$ both $\langle T|Z\rangle$ and $\langle Y_{OH}|Z\rangle$ are above the values predicted by the steady flamelet model at $\chi_q$, indicating that re-ignition has occurred. Also note that the ODT values of both $\langle T|Z\rangle$ and $\langle Y_{OH}|Z\rangle$ are larger than the DNS on at $Z \gtrapprox 0.45$ (rich side), indicating that the ODT model predicts a stronger re-ignition than DNS (note that at $\tau = 20$ the ODT model over-predicted extinction). Despite this quantitative disagreement, the qualitative trend of extinction followed by re-ignition, exhibited by DNS data, is captured by the ODT model. The RMS fluctuations in $T|Z$ and $Y_{OH}|Z$ at different time intervals are also compared with DNS data and included in the supplemental information. The trend exhibited by the ODT model is consistent with the DNS, although the fluctuations predicted by the model are lower than the DNS data.

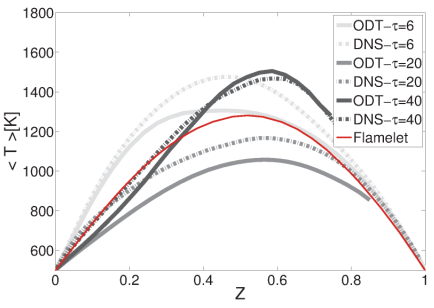


Figure 4: Conditional mean temperature, $\langle T|Z\rangle$, at $\tau = 6$, 20 and 40. The steady flamelet solution at $\chi_q$ is also shown for reference.

Figures 6 and 7 show evolution of the conditional probability density function (PDF) of $T$ and $\log_{10}\left(\chi/\chi_q\right)$ respectively

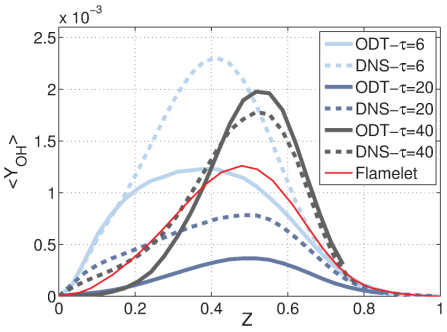


Figure 5: Conditional mean OH, $\langle Y_{OH}|Z\rangle$, at $\tau = 6$, 20 and 40. The steady flamelet solution at $\chi_q$ is also shown for reference.

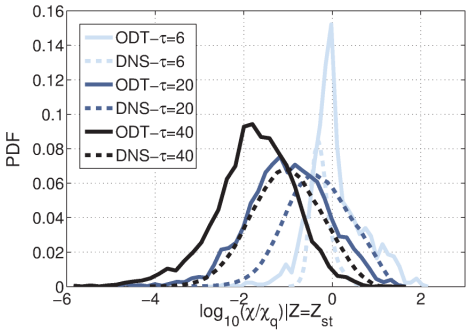


Figure 7: Conditional PDF of $\log_{10}\chi|_{Z_{st}}$ at $\tau = 6$, 20 and 40.

near $Z_{st} = 0.42$ at three different time intervals ($\tau = 6$, 20 and 40). In the early stages of the simulation (at $\tau = 6$), the scalar dissipation PDF evolution shows a narrower distribution and is shifted toward higher values relative to the DNS data. These higher values of $\chi$ cause extinction in the early stages of the ODT simulations, resulting in a corresponding temperature PDF shift toward lower values with the most probable state near the steady flamelet extinction limit of $T \approx 1250$ K. The higher $\chi$ predicted by ODT in the early stages of development is followed by a decrease in $\chi$ that is more rapid than exhibited by the DNS data. At $\tau = 20$ the mixing rates are still high enough to cause extinction in the model, as indicated by the tails of the PDF in Figure 7. During the later stages of the simulation ($\tau = 40$), mixing rates relax as indicated by the dissipation PDF shift toward lower values and the temperature PDF evolution starts shifting toward high values as reignition occurs.

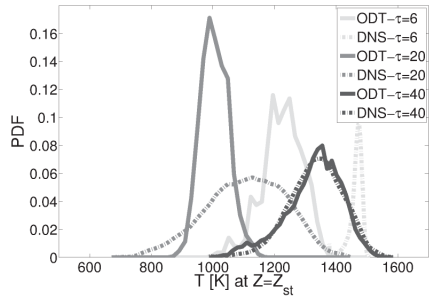


Figure 6: Conditional PDF of $T|_{Z_{st}}$ at $\tau = 6$, 20 and 40.

There are three different modes through which re-ignition can happen: autoignition, triple or edge flame propagation and turbulent flame folding [31]. The dominant re-ignition mechanism for the present case is turbulent flame folding [32, 33], where neighboring flame segments that are vigorously burning can provide a source for re-ignition. ODT can capture this mode of re-ignition because of triplet map action during an eddy event. The triplet map (10) instantly rearranges momentum and scalar fields enabling heat transfer from burning to non-burning regions. Since the domain is restricted to one dimension in ODT, the triple flame re-ignition mode (for which non-aligned gradients of mixture fraction and progress variable are needed [19]) cannot be addressed.

Figure 8 shows comparison of $\langle\chi|Z\rangle$ as a function of time for stoichiometric and fuel rich regions. The ODT model predicts higher $\langle\chi|Z\rangle$ (exceeding $\chi_q$), in the early stages, for both the regions compared to the DNS data, and as a result, early extinction occurs. In the fuel rich region $\langle\chi|Z\rangle$ starts increasing as the simulation starts and exceeds $\chi_q$ as early as $\tau = 2$ and starts decaying from $\tau = 3$, whereas the corresponding times for the stoichiometric region are 4 and 6, respectively. The DNS data also exhibits regions in which $\chi$ exceeds $\chi_q$ consistent with the model results; however the maximum mean $\chi$ occurs later than in the model, resulting in earlier occurrence of extinction by the model in the results reported thus far. In subsequent stages, the predicted $\langle\chi|Z\rangle$ is lower than the DNS data. However, extinction continues until $\tau = 20$ which is evident from Figure 6. In the later stages of the simulation, $\langle\chi|Z\rangle$ predicted by ODT is lower in both regions compared to the DNS data, indicating a faster increase towards equilibrium resulting in higher mean temperature and OH species concentration.

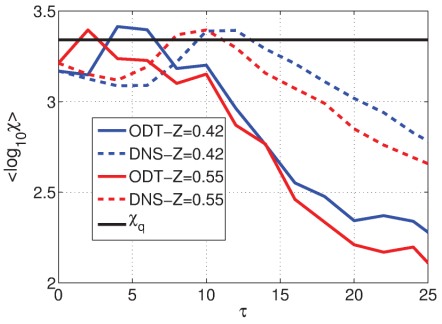


Figure 8: Evolution of $\log_{10}\langle\chi|Z\rangle$ with time (recall $Z_{st} = 0.42$). The horizontal line indicates the steady extinction limit, $\chi_q$.

Early extinction observed in the model is the primary reason for the discrepancies observed between the ODT and DNS data. In the ODT model, the large eddies control the flow entrainment [17], which is well captured by the model (see Figures 2 and 3), whereas small eddies influence the small-scale mixing. Because of the high shear available in the initial stages, the

UU IR Author Manuscript

eddy frequency is high. Implementation of an (instantaneous) eddy event further increases the strain rate within its interval, generating a turbulent cascade process (vortex stretching). For DNS, in the initial stages Kelvin-Helmholtz instabilities occur because of the high shear and significant velocity differences between fuel and oxidizer surface. Gradual growth in the size of coherent structures is observed for this case due to vortex pairing. Vortex pairing is inherently a multi-dimensional process that requires large structures at two different downstream locations to interact. The stand-alone ODT model cannot address this process because of its one-dimensional nature. This limitation of the model could help explain why early extinction occurs. As the simulation progresses, the strain rates become low and mixing rates relax. Once these rates relax the re-ignition take places as described above. Overall the model exhibits stronger extinction and re-ignition characteristics compared to the DNS data. LES combined with ODT as a subgrid model may better capture both large-scale amalgamation as well as small-scale mixing processes representative of extinction in reactive jets.

The present results may be compared with another recent effort to model this DNS flame that combined LEM with a three-dimensional LES and an artificial neural network approach to accelerate chemistry computation [27]. The results obtained in the present work are of comparable quality to those obtained in [27], with a significantly reduced computational effort. Interestingly, both works exhibit the same the key discrepancy with the DNS, *i.e.* the over-prediction of both the extinction and reignition processes.

## 5. Conclusions

In this paper, the ODT model is applied to a syngas jet flame, and direct comparison is made with DNS data. This study is first of its kind where a direct comparison has been made between ODT and 3D DNS data for a turbulent reacting flow. The present study focused on evaluating the model's ability to capture finite-rate-chemistry effects including extinction and reignition. A detailed comparison of jet spread rate as well as the thermochemistry for OH species has been presented. Results indicate that the ODT formulation can provide quantitatively accurate results for characteristic quantities of the jet such as spread rate and entrainment. Additionally, the ODT model can qualitatively capture both extinction and reignition that is exhibited by the DNS data.

The ODT calculations presented herein required approximately 2 hours per realization, and 400 realizations were used to provide well-converged statistics. Relative to DNS, ODT represents a very inexpensive modeling approach that can describe much of the physics present in the DNS, including PDF evolution, minor species evolution, finite-rate chemistry effects, *etc*. Indeed, these results, together with the body of previous work in ODT of reacting flows [17, 19, 20], suggest that ODT can provide reasonably accurate predictions for turbulent combustion, even as a stand-alone model.

Alternatively, ODT could be used as a means to identify reduced-order models for use in LES or RANS, as has been shown for nonreacting [13, 14, 34, 35] and reacting [18, 21, 22] cases.

Further adjustment/optimization of model parameters may result in better agreement for minor species between model prediction and DNS data. Future work will consider other DNS cases (Case L and H [25]) to examine the effects of Reynolds number on the ODT model parameters.

## 6. Acknowledgements

This material is based upon work supported by the Department of Energy under Award Number FC26-08NT0005015.

Work at Sandia was supported by the US Department of Energy, Office of Basic Energy Sciences, Division of Chemical Sciences, Geosciences and Energy Biosciences. Sandia is a multiprogram laboratory operated by Sandia Corporation, a Lockheed Martin Company, for the US Department of Energy under contract DE-AC04-94AL85000.

The DNS aspects of this research used computing resources of the National Center for Computational Sciences at Oak Ridge National Laboratory (NCCS/ORNL) which are supported by the Office of Science of the U.S. Department of Energy under contract number DE-AC05-00OR22725.

## References

[1] K. N. C. Bray, Proc. Combust. Inst. 26 (1996) 1–26.
[2] N. Peters, Turbulent Combustion, Cambridge University Press, Cambridge, UK, 2000.
[3] A. Kerstein, J. Fluid Mech. 231 (1991) 361.
[4] A. Kerstein, Combust. Flame 75 (1989) 397–413.
[5] A. Kerstein, J. Fluid Mech. 216 (1990) 411–435.
[6] P. A. McMurtry, S. Menon, A. R. Kerstein, Proc. Combust. Inst. 24 (1992) 271–278.
[7] S. Menon, P. McMurtry, A. R. Kerstein, in: B. Galperin, S. Orszag (Eds.), LES of Complex Engineering and Geophysical Flows, Cambridge University Press, Cambridge, 1993, pp. 287–314.
[8] V. Sankaran, S. Menon, Proc. Combust. Inst. 3 (2005) 575–582.
[9] A. R. Kerstein, J. Fluid Mech. 392 (1999) 277–334.
[10] W. T. Ashurst, A. R. Kerstein, Phys. Fluids 17 (2005).
[11] A. R. Kerstein, W. T. Ashurst, S. Wunsch, V. Nilsen, J. Fluid Mech. 447 (2001) 85–109.
[12] N. Krishnamoorthy, Reaction Models and Reaction State Parameterization for Turbulent Non-Premixed Combustion, Ph.D. thesis, University of Utah, 2008.
[13] R. C. Schmidt, A. R. Kerstein, S. Wunsch, V. Nilsen, J. Comp. Phys. 186 (2003) 317–355.
[14] R. C. Schmidt, R. J. McDermott, A. R. Kerstein, Comput. Methods Appl. Mech. Engrg. in press (2010).
[15] S. Wunsch, A. Kerstein, J. Fluid Mech. 528 (2005) 178–205.
[16] S. Wunsch, A. Kerstein, Phys. Fluids 13 (2001) 702–712.
[17] T. Echekki, A. R. Kerstein, T. D. Dreeben, Combust. Flame 125 (2001) 1083–1105.
[18] B. Ranganath, T. Echekki, Prog. Comput. Fluid Dynam. 6 (2006) 409–418.
[19] J. C. Hewson, A. R. Kerstein, Combust. Sci. Technol. 174 (2002) 35–66.
[20] J. C. Hewson, A. R. Kerstein, Combust. Theory Model. 5 (2001) 669–697.
[21] B. Ranganath, T. Echekki, Combust. Flame 154 (2008) 23–46.
[22] S. Cao, T. Echekki, J. Turbul. 9 (2008) 1–35.
[23] N. Punati, J. C. Sutherland, Application of an Eulerian One Dimensional Turbulence Model to Simulation of Turbulent Jets, U.S. Joint Sections of the Combustion Institute, Ann Arbor, MI, 2009.

[24] N. Punati, J. C. Sutherland, E. R. Hawkes, A. R. Kerstein, J. H. Chen, A Comparison of Direct Numerical Simulations with the One-Dimensional Turbulence Model for a Syngas Jet Flame, Western States Section of the Combustion Institute, Irvine, CA, 2009.
[25] E. R. Hawkes, R. Sankaran, J. C. Sutherland, J. H. Chen, Proc. Combust. Inst. 31 (2007) 1633–1640.
[26] E. R. Hawkes, R. Sankaran, J. H. Chen, S. A. Kaiser, J. H. Frank, Proc. Combust. Inst. 32 (2009) 1455–1463.
[27] B. Sen, E. Hawkes, S. Menon, Combust. Flame in press (2009).
[28] T. Echekki, A. R. Kerstein, J. C. Sutherland, Turbulent Combustion Modeling: Advances, New Trends and Perspectives, (in preperation) Springer.
[29] J. C. Sutherland, N. Punati, A Unified Approach to the Various Formulations of the One-Dimensional Turbulence Model, Technical Report, Insitute for Clean and Secure Energy, The University of Utah, 2010.
[30] R. W. Bilger, S. H. Stårner, R. J. Kee, Combust. Flame 80 (1990) 135–149.
[31] P. Sripakagorn, S. Mitarai, G. Kosaly, H. Pitsch, J. Fluid Mech. 518 (2004) 231–259.
[32] E. R. Hawkes, R. Sankaran, J. H. Chen, A Study of Extinction and Reignition Dynamics in Syngas Jet Flames Using Terascale Direct Numerical Simulations: Sensitivity to the Choice of Reacting Scalar, Proceedings of the Australian Combustion Symposium, 2007.
[33] E. R. Hawkes, R. Sankaran, J. H. Chen, Combust. Flame (in preparation).
[34] R. J. McDermott, A. R. Kerstein, R. C. Schmidt, P. J. Smith, J. Turbul. 6 (2005) 1–33.
[35] R. J. McDermott, Toward One-Dimensional Turbulence subgrid closure for Large-Eddy simulation, Ph.D. thesis, University of Utah, 2005.



UU IR Author Manuscript